2022 2nd International Conference on Advance Computing and Innovative Technologies in Engineering (ICACITE) | 978-1-6654-3789-9/22/$31.00 ©2022 IEEE | DOI: 10.1109/ICACITE53722.2022.9823893

A New improved NSST based Multimodal Medical Imaging System based on GWO and Image Enhancement with NLM Algorithm

[1] Dr. B. Rajalingam
Associate Professor
[1] Department of CSE
St. Martin's Engineering College,
Secunderabad, Telangana, India
rajalingam35@gmail.com

[2]Dr. R.Santhoshkumar
Associate Professor
Department of CSE
St. Martin's Engineering College,
Secunderabad, Telangana, India
santhoshkumar.aucse@gmail.com

[3]P. Deepan
Assistant Professor
Department of CSE (AI&ML)
St. Martin's Engineering College,
Secunderabad, Telangana, India
deepanp87@gmail.com

***Abstract*— Multimodal Medical fusion imaging is a salient feature not only in image-guided medical diagnosis but also treatment and various computer guided medical procedures. This paper proposes an efficient medical fusion imaging system that is evolved from the concept of Non-Subsampled Shearlet Transform (NSST) and the Gray Wolf Optimization (GWO) technique. Optimum decomposition level is determined by GWO technique and the optimum gain parameters. Finally, one more procedure is added to the entire procedure known as denoising and enhancement process is carried out to improve its visual quality and improve detailing. Work performance of these traditional fusion techniques are hampered greatly in cases when the images are corrupted with noise. Hence there is a need to develop a fusion technique that is capable of preserving precise information even when images are corrupted. It is also challenging to achieve suppressed noise and enhanced textural simultaneously. This proposed work is a study to compare traditional spatial, transform, filter and neural network domain fusion techniques with optimized NSST fusion imaging.**

Keywords*— Non-Subsampled Shearlet Transform (NSST), Gray Wolf Optimization (GWO), Histogram Matching, Non-Local Means Filter (NLM) and Multimodal medical image.

I. INTRODUCTION

Medical imaging has been the most critical and vital part of modern health care practices. Now a days, medical image processing is highly essential for patient management system starting from diagnosis to post-treatment analysis. The diagnosis of the disease involves non-invasive acquisition of information about the human body organs through imaging. There are many modalities available for capturing the data from affected part of the body. These are based on the physics used in the acquisition process. CT provides the information related to calcifications, bone structures, tumour outline prominently. MRI is predominant and most effective diagnostic procedure in assessing soft tissue anatomy. PET and SPECT images give abnormal metabolism at cancer infected tissues. Thus, every modality may not exhibit all the necessary information related to a particular dis ease. The acquisition of combined details regarding different modalities with a single machine is unavailable in almost all the health centres. The new PET- MRI scanner is under development stage [1]. Therefore, there is social and urgent need to have a software solution which will provide combined information from different imaging modalities in a single frame with the minimum cost. Such software solution is called Multimodality medical fusion imaging (MMIF) [2]. It is a process of creating new enriched single frame from two or more modality images with all the relevant and complementary information. It should also aid radiologist to get all the anatomical structures from both the modalities and provide better visualization of the abnormalities. As a result, global optimization has proven to be an effective strategy for identifying unconstrained maxima and minima for both continuous and differentiable functions, which makes it possible to provide the best solutions for a variety of problems [3]. These are also mostly used for upgrading the performance of fusion imaging methods by producing optimal transform fusion parameters and decomposition level. NSST fusion technique that have appropriate parameter values leads to producing and achieving upgraded fusion performance and finest quality of images. CFO and PSO are combined in Gray Wolf Optimization (GWO), which results in a memory with increased capacity, simpler usage, reduced process completion time (duration), increased convergence speed (speed of convergence) [5].

Rest of the paper comprises of the following sections. Section 2 states fundamentals of the NSST fusion method and GWO. Section 3 provides a detailed description regarding multimodal medical fusion imaging system. Section 4 states the evaluation metrics for utilized fusion quality. Section 5 states simulation results and comparisons done. Concluding remarks are described in Section 6.

II. EASE OF USE

A. *Non-sub Sampled Shearlet Transform (NSST)*

Geometric analysis now has a new multiple-scale tool in the form of NSST. There's a lot of potential here for recording 3-D geometry [6][7]. Moreover, it's a well-designed or well-representation of medical imagery. In compared to geometric analysis tools, this leads in NSST having the property of shift invariance as well as higher flexibility for directional selectivity. It is feasible to decompose the original multimodal medical image into a low-frequency sub-image and numerous high-frequency sub-images [8].

B. *Gray Wolfs Optimization*

The conventional Gray Wolfs Optimization algorithm for multimodal medical fusion imaging is described in this section. Newly developed swarm intelligence, GWO is derived from the idea of hunting mechanism used by the pack of gray wolves. The pseudocode of GWO technique has

been described in Fig. 2. Procedures involved in GWO are explained as follows.

a) Initializing positions of gray wolves: For the first and second modalities, the scale values [s1, s2] are taken into account in [0,1]. Limits for multimodal medical fusion imaging (MMFI) are 100 iterations and 100 scale values..

b) Initializing positions of gray wolves: Optimal selection of scale is carried out through GWO algorithm in multimodal medical fusion imaging. Mutual Information (MI) is measured quantitatively for multimodal medical fusion; this leads to providing information that is present in fused image. In this study, MI is considered a fitness function that is a maximization function, its purpose is to provide improved fusion assessment. Equation for MI is stated in Eq. (1).

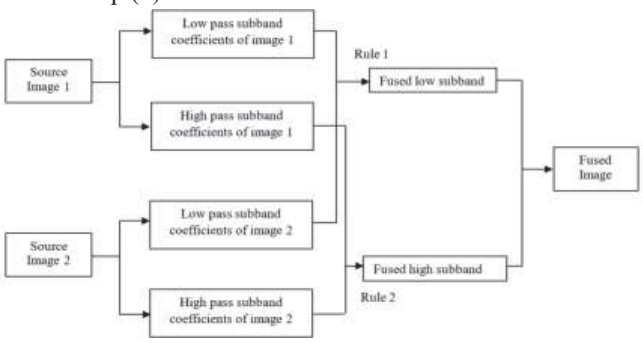

Fig. 1. Fusion process based on the NSST

$$MI(x,y) = \sum_x \sum_y p(x,y) log \frac{p(x,y)}{p(x)p(y)} \quad (1)$$

In Eq. (1), probability distribution function is denoted by P(x,y) and the marginal probability functions are denoted by P(x)and P(y) for both the modalities.

c) Assigning hierarchy among the gray wolves: Among the wildlife, gray wolves are always seen to remain in a pack and they possess good leadership qualities. A sum of 5–12 wolves complete the pack. There are four levels of hierarchy in this system: alpha (α), beta (β), delta (δ), and omega (ω). Alpha wolves are the pack's decision - makers and are responsible for making decisions on hunting, resting, waking, and sleeping times, as well as other aspects of life in the pack. Next in hierarchy are beta, these are known to be the best subordinates to alpha. The third is the delta wolf. They are expected to follow alphas and betas while they have dominance over omega wolves. The lowest hierarchical order is omega; these act as the scapegoat. Omega wolves are expected to follow upper three classification of wolves [10].

d) Encircling prey: The method adopted by the pack of gray wolves while hunting is encircling its prey before attacking it. Mathematical equations is stated in Eqs.(2) – (5).

$$\vec{D} = |\vec{C}.\overrightarrow{X_p}(t) - \vec{X}(t)| \quad (2)$$

$$\vec{X}(t+1) = \overrightarrow{X_p}(t) - \vec{A}.\vec{D} \quad (3)$$

$$\vec{A} = 2\vec{a}.\overrightarrow{r_1} - \vec{a} \quad (4)$$

$$C = 2.\overrightarrow{r_2} \quad (5)$$

Current iteration is denoted by t, vector position of prey is$\vec{X}_p$, $\vec{X}$indicates gray wolf position vector. Where $\vec{r}_1$and $\vec{r}_2$ are random vectors in the range [0,1], and an is a number that falls linearly from 2 to 0.

e) Hunting: The pack is capable of determining the location of its victim and, when the opportunity presents itself, encircling it completely. The alpha wolves are in charge of the majority of this hunts. Beta and delta wolves are used to assist in the hunting process. The alpha wolves are the most skilled hunters when it comes to determining the location of their prey. They are followed by beta and delta wolves. In terms of GWO, current iteration is forwarded by three finest search agents alpha, beta and delta, rest of the wolves in the pack are considered gamma. The numeric formulae are stated in Eqs.(6)–(8).

$$\vec{D}_\alpha = |\vec{C}_1.\vec{X}_\alpha - \vec{X}|, \vec{D}_\beta = |\vec{C}_2.\vec{X}_\beta - \vec{X}|, \vec{D}_\gamma = |\vec{C}_3.\vec{X}_\gamma - \vec{X}| \quad (6)$$

$$\vec{X}_1 = \vec{X}_\alpha - \vec{A}_1.(\vec{D}_\alpha), \vec{X}_2 = \vec{X}_\beta - \vec{A}_2.(\vec{D}_\beta), \vec{X}_3 = \vec{X}_\gamma - \vec{A}_3.(\vec{D}_\gamma) \quad (7)$$

$$\vec{X}(t+1) = \frac{\vec{X}_1 + \vec{X}_2 + \vec{X}_3}{3} \quad (8)$$

f) Attacking prey: When the prey comes to a complete stop, the moving grey wolves are able to successfully conclude their hunt by attacking the prey. While approaching the prey (according to mathematical standards), the grey wolves are required to reduce the value of $\vec{a}$, where an is reduced from 2 to 0 during the period of iterations.

g) Prey searching: Searching for prey is heavily dependent on the alpha wolf leaders, followed by beta and delta wolves. After then, they disperse to look for prey before reuniting to attack on the victim. A mathematical model of divergence is used to activate the search agent and diverge from the prey when values more than 1 or less than -1 are entered into the computation. Wolves encounter obstacles as they approach their prey, which prevents them from calmly attacking the prey swiftly, and this results in Vector C. Every search agent keeps track of the prey's distance from them [11].

III. METHODOLOGY

A. Procedural Steps for Proposed Optimized Multimodal Medical Fusion imaging System

1. Get two input multimodal medical images.
2. Adjust the size and register the multimodality medical images with the help of intensity-based image registration technique.
3. Histogram matching of a multimodal medical image 1 to a multimodal medical image 2.
4. The use of 2D NSST to obtain low-pass (LP) and high-pass (HP) coefficients for both the input medical images and the output medical images.
5. Initializing GWO in order to obtain gain parameters.
6. To get fused coefficients.
7. In order to get fused coefficients, the fusion process on LP and HP sub-bands is carried out with the help of a weighted average fusion rule with parameters (a1, b1) and (a2, b2), respectively, using the LP and HP sub-bands as inputs.

8. Implementation inverse non sub sampled shear let transform on coefficients to obtain estimation of the image fused.
9. Making sure that the fused images has the best possible metrics (such as local contrast, PSNR and entropy measures) before completing iterations.
10. Gain values updating of every corresponding decomposition level in case desirable solution is not obtained. This is achieved by maximising the local contrast, PSNR, and entropy metrics of the fused image.

Applying non local means filter algorithm for enhancement of the fused images.

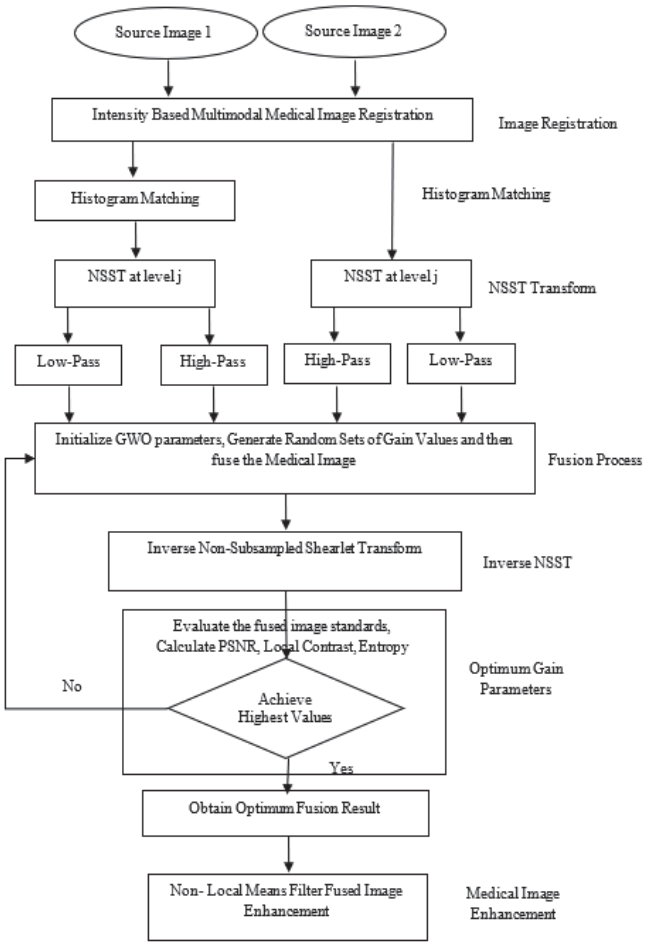

Fig. 2. Systemic representation of the proposed system for multimodality medical fusion imaging based on the NSST – GWO and Image Enhancement

Registration of an image is a vital processing multi-modality medical fusion imaging. This enables integrating the data attained from the images along with various modalities. In this paper the implemented registration algorithm is based on intensity of image registration. This schematic representation is described in Fig. 4. The figure summarizes the following points:

1. Applying a re-sample and a rigid, affine, or similarity transformation to images that are not aligned to each other.
2. Using reference images to evaluate the similarities.
3. Optimizing the transformation of the image after it has been aligned.
4. Using the similarity metric value to evaluate registration precision using landmark or feature definitions. Low-contrast image histogram matching is used to rectify a high-contrast image.

This step needs to be carried out in multi-modality fusion imaging because the ranges that are to be fused are varied [12].

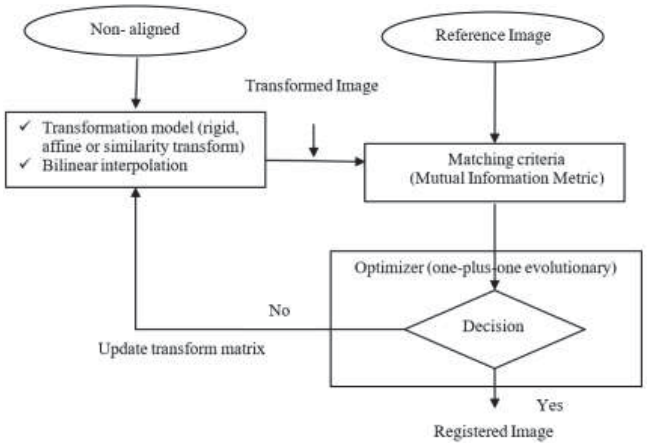

Fig. 3. An algorithm for intensity-based medical image registration

B. Local Contrast Enhancement Techniques

In order to de-noise an image the self-similarity assumption can be used. A similar neighborhoods pixel is useful in determining the denoised value of a pixel. Depending on the pixel reconstructed similarity, weights are assigned. Similarity assessment is done by considering the pixels and neigbhourhood. Mathematical equation is stated as below:

$$\mathrm{NL[u]}(x) = \frac{1}{c(x)} \int e^{-\frac{(G_a * |u(x+.) - u(y+.)|^2)(0)}{h^2}} u(y) dy \quad (14)$$

In the search window, integration is done over all pixels, where

$$c(x) = \int e^{-\frac{(G_a * |u(x+.) - u(y+.)|^2)(0)}{h^2}} u(y) dz \quad (15)$$

C (x) is referred to as a normalising constant. Ga denotes a Gaussian kernel, while h denotes a parameter for filtering.

C. Medical Fusion Imaging Quality Evaluation Metrics

Visual inspection is an important variable while evaluating the fused multimodality medical images. However, fusion quality evaluation can't completely depend on visual inspection alone. A comparison-based analysis of the presented fusion algorithm is carried out objectively and subjectively [13][14]. A complete quality assessment is done and is compared with several different traditional fusion techniques. Subjective and objective evaluation of this multi-modality medical fusion imaging system is done with the help of several metrics as listed below [15].

IV. Results and Discussions

An extensive series of simulation experiments was conducted to evaluate the performance of the optimised multimodality medical fusion imaging system under a variety of different environments. Findings of the experiment were obtained by running it in MATLAB R2017b on a

Windows 7 computer with 4.0 GB of RAM and an Intel Core I5 processor, and the results are provided in Table 1. We used online datasets from Harvard Medical School [16] and Radiopedia.org [17] to compile the multimodal medical images. Scaling each image down to 256 256 and 512 512 pixels completes the process. Various medical images are among the datasets being examined for its ability to identify Alzheimer's disease, Anaplastic Astrocytoma, and Degenerative Disease. These images were subjected to a variety of treatments in order to achieve the intended outcome. Medical images are registered, histogram-matched, optimally fused, and enhanced before the last phase of image enhancement is conducted. This system's implementation begins with the registration of images.

This is a crucial step that includes adjusting data set images to equalized sizes, uniform orientation, and alignment boundaries. This step helps in providing enhanced information to accurately match fusion process to improve quality of fused images. Histogram matching is carried out to match the varied images ranges to be fused. Along with the NSST fusion procedure GWO process also takes place for optimizing the fusion gains. At the end, a post processing procedure is carried out to improve the contrast. Results obtained by optimized NSST fusion technology is compared to the results of the PCA, DWT, Curvelet, Guided Filtering, PCNN, DFRWT and NSCT fusion techniques. Generally, the performance of a fusion technique can't be determined only based on few definite metrics. Therefore, several evaluation metrics are combined to estimate the fusion quality. Hence, this proposed multimodal medical fusion imaging technique is evaluated both subjectively and objectively using multiple performance evaluation metrics. As shown in Figures 4 and Figure 10, the MRI and SPECT data of Alzheimer's disease patients, those with Alzheimer's disease-related anplastic astrocytoma, and those with moderate alzheimer's disease are all shown (MRI & PET). Figures 5, 6, 8, 9, 11, and 12 show the input images a and b, the fused images c, d, e, f, and g, respectively, and the fused images h and j, respectively.

A. Fusion imaging of MR and SPECT

In this section, we'll take a look at two real-life examples of MR and SPECT imaging combined for medicinal purposes. For the first case, a 73-year-old woman with Alzheimer's disease was evaluated by a neuropsychologist because she had been losing her memory for three years, and for the second, a 51-year-old woman with anaplastic atrocytoma had to be evaluated because she had been losing her vision in her right eye (visual loss). As can be seen in Figures 5, 6, 8 and 9 the NSST-GWO is used to combine MR and SPECT pictures in this region.

B. Fusion imaging of MR and PET

This section contains fusion analysis of MR and PET images obtained from the medical circumstances listed below. Grand male seizure and escalating speech difficulties were observed in the first instance, involving a 50-year-old man with grade 4 mild Alzheimer's disease, and in the second case, an elderly man with mild Alzheimer's disease, grade 2 mild Alzheimer's disease, experienced a grand male seizure. Figures 11 and 12 show the scanned medical photos that were used in the analysis. Both the anatomical MR structure and the functional PET are plotted.

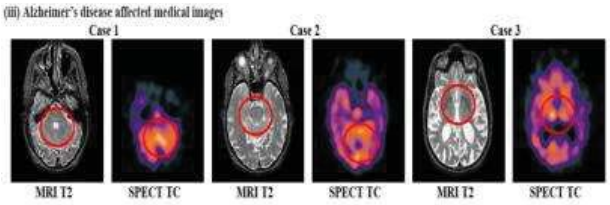

Fig. 4. Three set of Alzheimer's disease affected input images

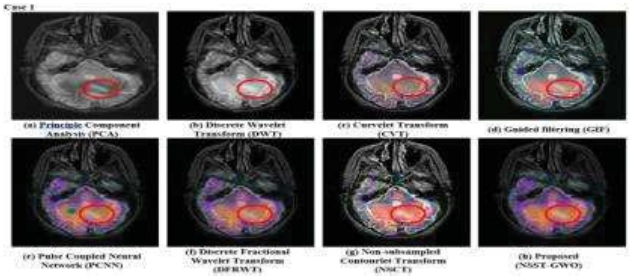

Fig. 5. Experimental results of the alzheimer's disease

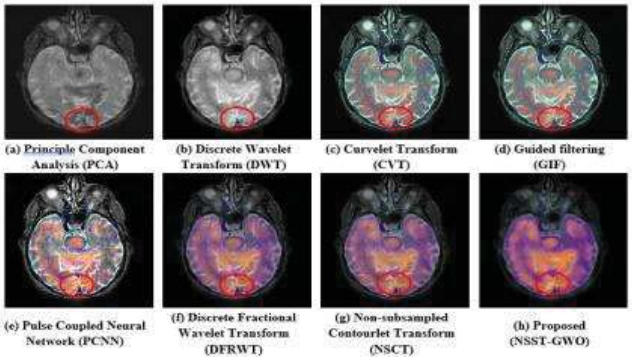

Fig. 6. disease-related changes in case 2's medical images

TABLE I. COMPARISON OF DIFFERENT FUSION IMAGING METHODS ON IMAGES IMPACTED BY ALZHEIMER'S DISEASE

Set	Methods	PCA	DWT	CVT	GIF	PCNN	DFRWT	NSCT	Proposed (NSST-GWO)
Case 1	Fusion Factor	2.168	2.334	2.854	2.985	3.231	3.487	3.672	**4.192**
	Mutual Information	2.487	2.743	2.876	2.906	2.913	3.032	3.254	**3.965**
	Cross Entropy	1.996	1.963	1.863	1.832	1.528	1.476	1.402	**1.025**
	Standard deviation	39.65	42.42	44.09	43.76	46.51	49.05	50.76	**59.76**
	PSNR	50.04	55.65	60.98	62.45	62.98	63.58	30.56	**68.06**
	Process completion time (sec)	90.42	87.61	106.6	130.0	84.39	80.54	76.43	**68.56**
Case 2	Fusion Factor	2.053	2.562	3.012	3.326	3.576	3.675	3.984	**4.763**
	Mutual Information	3.187	3.065	3.231	3.346	3.391	3.476	3.572	**3.896**
	Cross Entropy	1.395	1.285	1.128	1.017	1.382	1.294	1.005	**0.951**
	Standard deviation	43.07	44.87	48.95	45.65	47.86	49.99	52.75	**65.98**
	PSNR	45.76	48.98	56.98	59.73	60.32	49.98	36.65	**63.95**
	Process completion time (sec)	87.81	95.41	99.01	120.3	84.46	93.61	78.21	**65.68**

Fig. 6 shows how the disease-related changes in case 2's medical images were observed in an experiment. Table 1 shows the results of a comparison of different fusion imaging methods on images impacted by Alzheimer's disease.

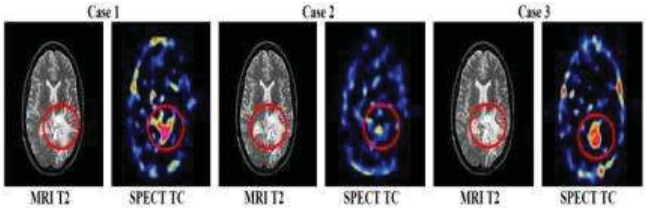

Fig. 7. Three set of Anaplastic Astrocytoma disease affected input images

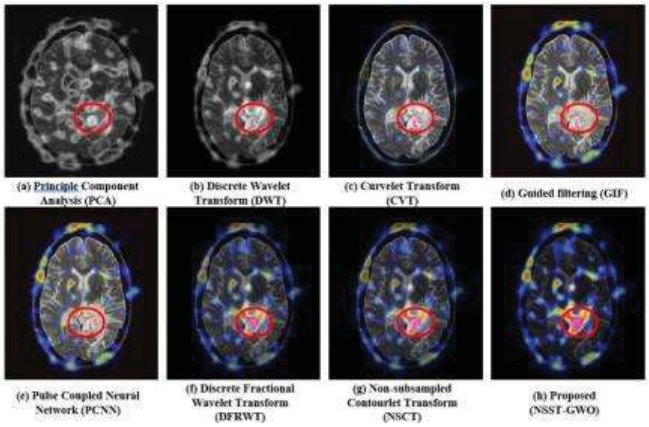

Fig. 8. Anaplastic astrocytoma experimental results in medical images for case 1

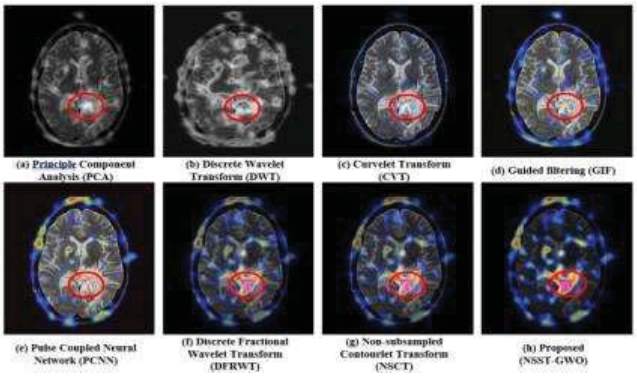

Fig. 9. Anaplastic astrocytoma experimental results in medical images for case 2

TABLE II. COMPARISON OF DIFFERENT FUSION IMAGING METHODS ON IMAGES IMPACTED BY ALZHEIMER'S DISEASE

Set	Methods	PCA	DWT	CVT	GIF	PCNN	DFRWT	NSCT	Proposed (NSST-GWO)
Case 1	Fusion Factor	2.487	2.893	2.918	3.065	3.154	3.198	3.276	**4.186**
	Mutual Information	2.065	2.176	2.255	2.263	2.387	2.398	2.538	**2.975**
	Cross Entropy	2.487	2.317	2.276	2.102	2.386	1.905	2.023	**1.376**
	Standard deviation	40.56	42.52	41.06	43.45	43.65	45.32	45.52	**48.64**
	PSNR	38.82	39.53	41.57	40.58	42.03	44.82	33.76	**61.67**
	Process completion time (sec)	99.65	86.58	79.08	114.0	80.35	85.98	98.56	**74.47**
Case 2	Fusion Factor	1.168	1.234	1.854	1.985	2.041	2.487	2.677	**3.156**
	Mutual Information	1.447	1.773	2.866	2.924	2.813	3.105	3.321	**3.704**
	Cross Entropy	2.696	2.963	2.861	2.532	2.328	2.176	2.029	**1.235**
	Standard deviation	32.38	35.40	39.03	41.48	43.10	47.05	53.03	**57.05**
	PSNR	41.04	47.61	49.98	50.42	54.98	59.51	57.12	**65.46**
	Process completion time (sec)	95.62	86.20	89.65	97.23	90.43	80.69	94.40	**79.60**

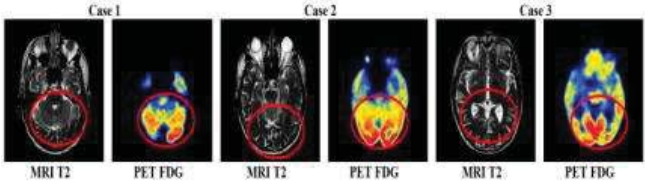

Fig. 10. Three set of mild alzheimer's disease affected input images

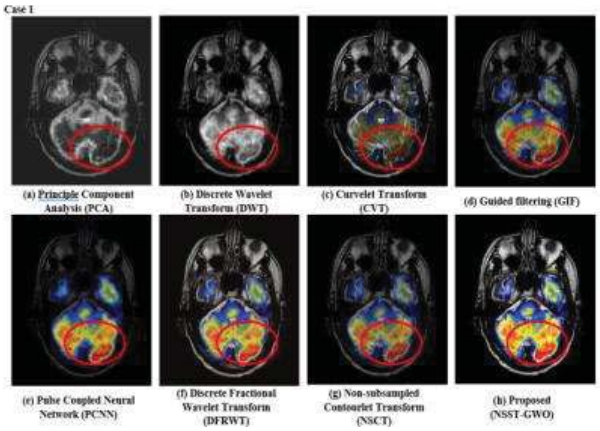

Fig. 11. Mild Alzheimer's disease damaged medical images for case 1

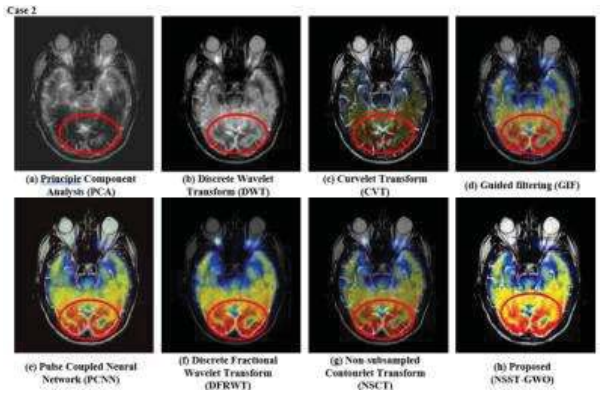

Fig. 12. Mild Alzheimer's disease damaged medical images for case 2

Here, the optimized NSST fusion technique with an attempt to address the issues faced by the conventional fusion technologies. For this purpose, the proposed optimized medical fusion imaging technique must be compared with the conventional fusion methods. Tables 1, 2 and 3 illustrate that traditional fusion techniques are capable of achieving good cross entropy, PSNR, and quality metrics. However, they are not efficient in providing efficient images because of factors such as decreased standard deviation values, fusion factor and Mutual information. Superior performance can be obtained by selecting the following variables. Hence these fusion systems enhance the quality of image by escalating average gradient values and improve detailing. The high edge intensity values of this medical imaging technique are extra detailed. Moreover, greater standard deviation values lead to improved images results. A surprising characteristic of the GWO method used in this proposed technique is used to obtain optimum gain parameters at varied decomposition levels. These factors make this system most appropriate for real-time applications. Figure 13, 14 and 15 shows the contrast enhanced output images using NLM algorithms.

TABLE III. EVALUATIONS OF FUSION IMAGING ALGORITHMS IN THE CASE OF DEGENERATIVE DISEASE AFFECTED IMAGES

Set	Methods	PCA	DWT	CVT	GIF	PCNN	DFRWT	NSCT	Proposed (NSST-GWO)
Case 1	Fusion Factor	2.168	2.234	2.854	2.985	3.041	3.487	3.777	**4.456**
	Mutual Information	2.447	2.573	2.836	2.954	2.805	2.905	3.021	**3.841**
	Cross Entropy	3.696	3.863	3.904	3.532	3.324	3.176	3.029	**1.754**
	Standard deviation	39.38	35.41	40.10	41.50	44.28	45.07	49.41	**56.10**
	PSNR	45.29	47.40	49.34	51.41	53.91	55.55	57.69	**64.41**
	Process completion time (sec)	100.3	89.20	78.65	99.34	90.78	80.90	93.30	**75.30**
Case 2	Fusion Factor	3.053	3.565	3.298	3.347	3.586	3.630	3.792	**4.356**
	Mutual Information	2.187	2.067	2.234	2.346	2.394	2.475	2.570	**2.892**
	Cross Entropy	2.395	2.285	2.128	2.017	2.384	1.993	1.895	**1.251**
	Standard deviation	41.59	43.84	46.20	48.62	50.82	49.02	51.39	**62.45**
	PSNR	39.71	40.21	45.91	50.73	51.51	54.01	59.01	**62.40**
	Process completion time (sec)	85.32	80.40	78.01	110.2	90.20	94.10	78.18	**73.49**

(a) Proposed fused output image (b) Contrast Enhance output image

Fig. 13. Contrast Enhanced Alzeimer's disease affected output images

(a) Proposed fused output image (b) Contrast Enhanced output image

Fig. 14. Contrast Enhanced Degenerative disease affected output images

(a) Proposed fused output image (b) Contrast Enhanced output image

Fig. 15. Contrast Enhanced Anaplastic astrocytoma disease affected output images

At the end, for evaluation and testing of the post-processing, comparisons have been carried out among various local contrast enhancement methods. These are carried out to perform the following functions: enhancing the fused image by refining the local contrast in order to obtain better image standards, add detailing to achieve the finest performance and the great visual output for precise and exact medical diagnosis and decide the interventions.

V. CONCLUSION

The paper has successfully proposed an absolute fusion imaging system for multimodality medical images with the help of NSST, GWO, and histogram processing. For achieving the fusion with the gain parameter measures, the system presents LP and HP sub-bands. This results in improvement of image standards along with quick processing period. Adding details for efficient medical diagnosis is obtained by local contrast enhancement techniques which are used on the fused images. Hence it is believed that this proposed technique will be an acceptable intervention for medical fusion imaging related constraints. Furthermore, NSST-GWO has shown superior results by fusing the medical images within less process completion times with better precision and hence, this proposed medical fusion imaging system can appropriately use in day-to-day clinical setting.

REFERENCES

[1] A. James, Belur V. Dasarathy, "Medical fusion imaging: A survey of the state of the art, Information Fusion", Elsevier, Vol. 19, pp.4–19, 2015.

[2] D. Gupta, "Nonsubsampled shearlet domain fusion techniques for CT–MR neurological images using improved biological inspired neural model", Biocybernetics and Biomedical Engineering, Vol. 1(3), pp. 1-12, 2012.

[3] E. Daniel, "Optimum Wavelet Based Homomorphic Medical Fusion imaging Using Hybrid Genetic – Gray Wolf Optimization Algorithm", IEEE Sensors Journal, Vol. 1(4), pp.1558-1748, 2018.

[4] E. Daniel, J. Anithaa, K.K Kamaleshwaran, I. Rani, "Optimum spectrum mask based medical fusion imaging using Gray Wolf Optimization", Biomedical Signal Processing and Control, Elsevier, Vol. 34, pp. 36 – 43, 2017.

[5] H.M. El-Hoseny, E.M. Rabaie, W. Elrahman, F.E. Samie, "Medical Fusion imaging Techniques Based on Combined Discrete Transform Domains", 34th National Radio Science Conference, Port Said, Egypt, Arab Academy for Science, Technology & Maritime Transport, IEEE, pp. 471-480, 2016.

[6] J. Du, W. Li, K. Lu, B. Xiao, "An Overview of Multi-Modal Medical Fusion imaging Algorithm in NSST Domain", Journal of Digital Imaging, Springer, pp. 121-130, 2015.

[7] J. Xi, Y. Chen, A. Chen, W. Chen, Medical Fusion imaging Based on Sparse Representation and PCNN in NSCT Domain", Computational and Mathematical Methods in Medicine, Hindawi, 2018.

[8] K.N. Narasimha Murthy, J. Kusuma, "Fusion of Medical Image Using STSVD", Proceedings of the 5th International Conference on Frontiers in Intelligent Computing: Theory and Applications, Advances in Intelligent Systems and Computing, Springer, Vol. 5(16), pp. 69-79, 2016.

[9] H.M. El-Hoseny, W. Abd El-Rahman, E.M. El-Rabaie, F.E. Abd El-Samie, O.S. Faragallah, "An Efficient DT-CWT Medical Fusion imaging System Based on Modified Central Force Optimization and Histogram Matching", Infrared Physics & Technology, Elsevier, Vol. 94, pp. 223-231, 2018.

[10] N. Ling, D. Mei-Xia, "Fusion for Medical Images based on Shearlet Transform and Compressive Sensing Model", International Journal of Signal Processing, Image Processing and Pattern Recognition, Vol.9, No.4, pp.1-10, 2018.

[11] P. Ganasala, V. Kumar, "Feature-Motivated Simplified Adaptive PCNN Based Medical Fusion imaging Algorithm in NSST Domain", J Digit Imaging, Springer, 2015.

[12] S. Satishkumar, S. Chavan, A. Mahajan, N. Sanjay, S. Desai, M. Thakur, A. D'cruz, "Nonsubsampled rotated complex wavelet transform (NSRCxWT) for medical fusion imaging related to clinical aspects in neurocysticercosis", Computers in Biology and Medicine, Elsevier, Vol. 81, pp. 64–78, 2017.

[13] S. Dileepkumar, J. Sachdeva, C. Kamal Ahuja, N. Khandelwal, "Multimodal medical fusion imaging using non-subsampled shearlet transform and pulse coupled neural network incorporated with morphological gradient", Signal, Image and Video Processing, Springer, 2018.

[14] L. Shuaiqi, S. Mingzhu, Z. Zhihui, J. Zhao, "Fusion imaging based on complex-shearlet domain with guided filtering", Multidim Syst Sign Process, Springer, 2016.

[15] S. Sneha, D. Gupta, R.S. Anand, V. Kumar, "Nonsubsampled shearlet based CT and MR medical fusion imaging using biologically inspired spiking neural network", Biomedical Signal Processing and Control, Elsevier, Vol. 18, pp. 91–101, 2015.

[16] https://radiopaedia.org , 2005

[17] http://www.med.harvard.edu (Accessed 2017)